Capillarity

Vol. 5, No. 6, p. 115-122, 2022

Original article

# Modeling of counter-current spontaneous imbibition in independent capillaries with unequal diameters

Kangli Chen[1,2], Huaxin Xu[1,2], Zhenjie Zhang[1,2], Qingbang Meng[1,2]*, Tao Zhang[3]

[1]*Key Laboratory of Theory and Technology of Petroleum Exploration and Development in Hubei Province, China University of Geosciences, Wuhan 430074, P. R. China*

[2]*School of Earth Resources, China University of Geosciences, Wuhan 430074, P. R. China*

[3]*Physical Science and Engineering Division, King Abdullah University of Science and Technology, Thuwal 23955-6900, Saudi Arabia*

**Keywords:**
Independent capillary model
counter-current imbibition
fluid viscosity
heterogeneity

**Cited as:**
Chen, K., Xu, H., Zhang, Z., Meng, Q., Zhang, T. Modeling of counter-current spontaneous imbibition in independent capillaries with unequal diameters. Capillarity, 2022, 5(6): 115-122.
https://doi.org/10.46690/capi.2022.06.02

**Abstract:**
Spontaneous imbibition is a crucial process for oil recovery from fractured and unconventional reservoirs. Herein, with the assumption of capillaries being independent, a new mathematical model for spontaneous imbibition is proposed and solved using a numerical method. The simulated results show that the wetting phase preferentially enters smaller capillaries where the advancement velocity is higher than that in larger ones, while the non-wetting phase can be displaced out in the larger capillaries. In addition, the effect of fluid viscosity ratio on counter-current imbibition is analyzed. The results show that imbibition velocity becomes higher with the increase in the viscosity ratio. When the viscosity of the non-wetting phase is larger than that of the wetting phase, the end pressure gradually increases as the imbibition front advances. In contrast, when the viscosity of the non-wetting phase is less than that of the wetting phase, the end pressure decreases with the infiltration. With a higher viscosity ratio of non-wetting and wetting phase, the heterogeneity of the interface advancement among different capillaries increases.

## 1. Introduction

When porous media suck in wetting phase fluid and discharge non-wetting phase fluid owing to the presence of capillary pressure, this phenomenon is called imbibition (Morrow and Mason, 2001; Cai et al., 2021). The essence of imbibition is the change in interface energy, which is expressed in the form of capillary pressure (Shen et al., 2020). The contact mode between porous media and fluid is known as the boundary condition of imbibition (Haugen et al., 2014). The contact modes between porous media and wetting and non-wetting phases are complex and diverse, resulting in the diversity of infiltration boundary conditions (Zhang et al., 1996; Xiao et al., 2019; Gong et al., 2021). Overall, the infiltration boundary conditions can be divided into single boundary and mixed boundary (Pooladi-Darvish and Firoozabadi, 2000). In the former case, the open surface of porous media is completely covered by the wetting phase fluid (Mason et al., 2010). By comparison, under the mixed boundary condition, the open surface of porous media partially contacts the wetting phase fluid as well as the non-wetting phase fluid (Qin et al., 2022). Imbibition can generally be divided into two modes: co-current imbibition and counter-current imbibition (Bourblaux and Kalaydjian, 1990). When the non-wetting phase fluid is discharged through the contact surface between porous medium and wetting phase fluid, it is called counter-current imbibition. In this case, the discharge of non-wetting phase needs to overcome capillary back pressure (Unsal et al., 2007; Nooruddin and Blunt, 2016; Foley et al., 2017). In co-current imbibition, non-wetting phase fluid is discharged through the contact surface between the porous medium and the non-wetting phase fluid. As a result, the

Yandy Scientific Press

*Corresponding author.
*E-mail address*: chen.kl@cug.edu.cn (K. Chen); huaxin_xu@163.com (H. Xu); zhenjiezhang1996@163.com (Z. Zhang); 13661645446@163.com (Q. Meng); tao.zhang.1@kaust.edu.sa (T. Zhang).

Received September 20, 2022; revised October 22, 2022; accepted November 9, 2022; available online November 13, 2022.

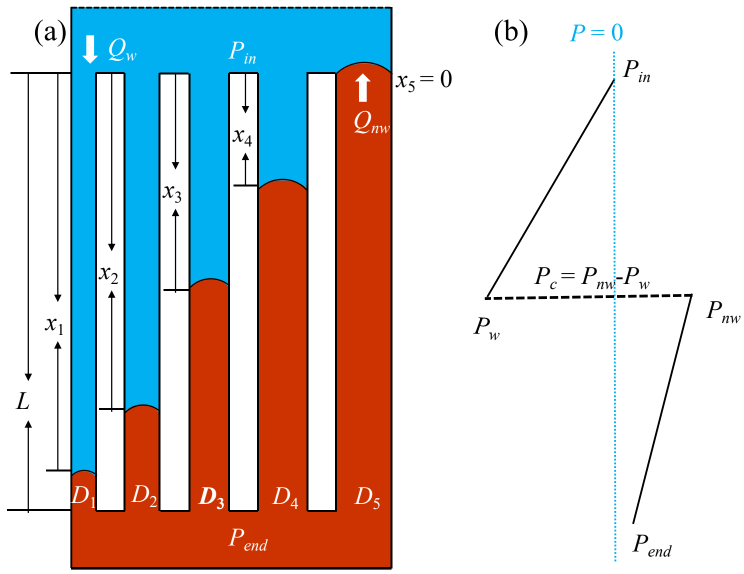


**Fig. 1**. Schematic diagram (a) and pressure distribution (b) of counter-current infiltration in five independent capillaries with different diameters.

discharge of non-wetting phase does not need to overcome the capillary back pressure (Meng et al., 2017a; Wang et al., 2021). For a single boundary condition, the non-wetting phase can only be discharged through counter-current imbibition (Abd et al., 2019; Zhou et al., 2019). For mixed boundary conditions, however, the non-wetting phase can be discharged by both co- and counter-current imbibition, although the majority of the production is driven by co-current imbibition (Mason and Morrow, 2013).

The capillary bundle model is often used to study the mechanism of imbibition because of its simple and intuitive characteristics (Wang and Dong, 2011; Cai et al., 2014; Gorce et al., 2016; Zhao et al., 2021). For a single capillary, the imbibition rate depends on capillary pressure and flow resistance (Kim et al., 2021; Cheng et al., 2022). Specifically, the capillary pressure is inversely proportional to the capillary radius, and the flow resistance is inversely proportional to the square of the capillary radius. Considering the effects of both, the smaller the capillary radius, the slower the infiltration rate. Macroscopically, the lower the permeability, the slower the imbibition (Meng et al., 2017b; Yang et al., 2019). In the early stage of research, Washburn (1921) used a single capillary to study the migration characteristics of gas-water two-phase interface, obtained the analytical equation of interface migration by a theoretical derivation method, and established the classical Lucas-Washburn imbibition equation, that is, the amount of imbibition is directly proportional to the square root of imbibition time (Washburn, 1921). Cai et al. (2010) established a co-current imbibition mathematical model based on fractal theory while considering the influence of tortuosity. Cai and Yu (2011) proposed that the imbibition index is not always equal to 0.5 and is also related to the tortuosity of the porous media. Dong et al. (2005, 2006) and Wang et al. (2011) established idealized connected capillary models with mixed boundary conditions. Due to the interconnection among the capillaries, the larger capillary pressure in smaller capillaries will form a resistance effect on the fluid flow in larger capillaries, resulting in a higher propulsion speed of the two-phase interface in smaller capillaries.

At present, most of the modelling work on capillary imbibition is focused on co-current imbibition, while less research has targeted the counter-current imbibition phenomenon. Due to its simple and intuitive characteristics, the capillary model has been an effective tool to characterize the behaviour and study the mechanism of counter-current imbibition. Meanwhile, based on the infiltration characteristics of the capillary model, it can better explain the macro-phenomenon of counter-current imbibition and provide a theoretical basis for the study of infiltration. With a focus on the independent capillary model, this paper proposed the mathematical model of capillary model, followed by the analysis of the velocity characteristics of counter-current imbibition. The effect of fluid viscosity ratio on the imbibition process is principally investigated.

## 2. Mathematical model of imbibition in five capillaries

In this work, five independent cylindrical capillary tubes are initially filled with non-wetting phase fluid. The influence of gravitational force is ignored. The outer ends of the capillaries contact the wetting phase directly, while the other ends of the capillaries are closed. Due to the capillary force, the capillary spontaneously absorbs the wetting phase without external force, and the non-wetting phase will be displaced from the larger capillaries. The schematic diagram of fluid distribution and pressure distribution in the capillary during infiltration is shown in Fig. 1.

It is assumed that single-phase flow in any tube is described by the Hagen-Poiseuille formula (Ruth and Bartley, 2002;

Gong and Piri, 2020):

$$Q_\alpha = \frac{\pi r_\alpha^4}{8\mu_\alpha}\frac{\mathrm{d}P_\alpha}{\mathrm{d}x} \tag{1}$$

where $\alpha$ represents the phase index, $Q$ is the fluid rate; $r$ is the capillary radius; $P$ is the pressure; $\mu$ is the viscosity; $x$ is the distance from the penetration leading edge to the inlet end. The flow rates of wetting phase and non-wetting phase in each capillary are equal. The flow rate in each capillary is obtained by describing the flow rate of wetting and non-wetting phases in their corresponding region, as:

$$Q_i = \frac{\pi r_i^4 (P_{in} - P_{wi})}{8\mu_w x_i} = \frac{\pi r_i^4 (P_{nwi} - P_{end})}{8\mu_{nw}(L - x_i)} \tag{2}$$

where the subscript $i$ represents the $i^{\text{th}}$ capillary; $P_{in}$ is the inlet pressure of wetting phase; $P_{end}$ is capillary end pressure; $P_{wi}$ and $P_{nwi}$ are the pressure of wetting phase and non-wetting phase at the interface; $\mu_w$ and $\mu_{nw}$ are the viscosity of wetting phase and non-wetting phase; $L$ is the capillary length.

We assume that the direction of the wetting phase entering the capillary is positive, i.e., $Q_i > 0$, and the direction of non-wetting phase discharging from capillary is negative, i.e., $Q_i < 0$.

The capillary pressure is equal to the difference between non-wetting phase pressure and wetting phase pressure at the imbibition front, as:

$$P_{ci} = P_{nwi} - P_{wi} \tag{3}$$

where $P_{ci}$ is the capillary pressure of the $i^{\text{th}}$ capillary.

Finally, from the law of conservation of mass:

$$\sum_{i=1}^{5} Q_i = 0 \tag{4}$$

Without considering the effect of gravity, a model of spontaneous imbibition with five capillaries is established using the Hagen-Poiseuille expression, capillary pressure formula and mass conservation law.

## 3. Solution of mathematical model

It is known that the diameters of the five capillary tubes are $D_1$, $D_2$, $D_3$, $D_4$, and $D_5$ respectively, the length of the five capillary tubes is $L$, the viscosity of the wetting phase and non-wetting phase fluid is $\mu_w$ and $\mu_{nw}$, respectively, the interfacial tension of the wetting phase and non-wetting phase is $\sigma$, and the pressure at the inlet of the capillary wetting phase is $P_{in}$. Based on these known parameters, the numerical method is used to solve the model.

The capillary pressure is calculated according to the following formula:

$$P_{ci} = \frac{2\sigma\cos\theta}{r_i} \quad (1 \le i \le 5) \tag{5}$$

where the contact angle $\theta$ is 0 in this work, $\sigma$ is the interfacial tension between wetting phase and non-wetting phase.

Assuming that the time step is $n$, the advancement distances of wetting phase in the capillary are $x_1^n$, $x_2^n$, $x_3^n$, $x_4^n$ and $x_5^n$, respectively. According to the advancement distance, the below solution derivation is made.

For the first capillary, Eq. (6) can be obtained according to Eq. (3), then Eq. (6) can be substituted into Eq. (2) to obtain Eq. (7). Finally, Eq. (8) of $P_{nwi}$ represented by $P_{end}$ can be obtained:

$$P_{wi} = P_{nwi} - P_{ci} \tag{6}$$

$$\frac{\pi r_i^4 (P_{in} + P_{ci} - P_{nwi})}{8\mu_w x_i^n} = \frac{\pi r_i^4 (P_{nwi} - P_{end})}{8\mu_{nw}(L - x_i^n)} \tag{7}$$

$$P_{nwi} = \frac{\mu_w x_i^n P_{end} + \mu_{nw}(L - x_i^n)(P_{in} + P_{ci})}{\mu_w x_i^n + \mu_{nw}(L - x_i^n)} \tag{8}$$

Substituting Eq. (8) into Eq. (2) can yield the formula of $Q_i$ represented by $P_{end}$:

$$Q_i = \frac{\pi r_i^4 (P_{nwi} - P_{end})}{8\mu_{nw}(L - x_i^n)} = \frac{\pi r_i^4 (P_{in} + P_{ci} - P_{end})}{8\mu_w x_i^n + 8\mu_{nw}(L - x_i^n)} \tag{9}$$

The derived Eq. (9) is substituted into the law of conservation of mass Eq. (4) to obtain Eq. (10), as:

$$\begin{aligned} &\frac{\pi r_1^4 (P_{in} + P_{c1} - P_{end})}{8\mu_w x_1^n + 8\mu_{mw}(L - x_1^n)} + \frac{\pi r_2^4 (P_{in} + P_{c2} - P_{end})}{8\mu_w x_2^n + 8\mu_{nw}(L - x_2^n)} + \\ &\frac{\pi r_3^4 (P_{in} + P_{c3} - P_{end})}{8\mu_w x_3^n + 8\mu_{nw}(L - x_3^n)} + \frac{\pi r_4^4 (P_{in} + P_{c4} - P_{end})}{8\mu_w x_4^n + 8\mu_{nw}(L - x_4^n)} + \\ &\frac{\pi r_5^4 (P_{in} + P_{c5} - P_{end})}{8\mu_w x_5^n + 8\mu_{nw}(L - x_5^n)} = 0 \end{aligned} \tag{10}$$

The formula for solving the pressure $P_{end}$ at the bottom of the non-wetting phase in the capillary at the $n^{\text{th}}$ time step can be obtained as:

$$a_i = \frac{r_i^4}{\mu_w x_i^n + \mu_{nw}(L - x_i^n)} \quad (i = 1, 2, 3, 4, 5) \tag{11}$$

Eq. (11) is used to simplify and solve Eq. (10).

$$P_{end} = \frac{a_1(P_{in}+P_{c1}) + a_2(P_{in}+P_{c2}) + a_3(P_{in}+P_{c3}) + a_4(P_{in}+P_{c4}) + a_5 P_{c5}}{a_1 + a_2 + a_3 + a_4 + a_5} \tag{12}$$

According to Eq. (12), $P_{end}$ can be calculated. Then, based on Eqs. (8) and (9), the pressure of the non-wetting phase fluid ($P_{nw1}$, $P_{nw2}$, $P_{nw3}$, $P_{nw4}$ and $P_{nw5}$) and the fluid flow rate ($Q_1$, $Q_2$, $Q_3$, $Q_4$ and $Q_5$) can all be calculated.

After obtaining the flow rate of each section of the capillary, the flow velocity of each capillary at the $n^{\text{th}}$ time step can be obtained according to the formula:

$$v_i^n = \frac{Q_i}{\pi r_i^2} \tag{13}$$

Based on the $n^{\text{th}}$ time step, the time increase is $\Delta t$. At this time, the model is in the $(n+1)^{\text{th}}$ time step, and the total time is:

$$t_{n+1} = t_n + \Delta t \tag{14}$$

On the basis that $\Delta t$ is infinitely close to 0, the velocity at this time can follow the velocities ($v_1^n$, $v_2^n$, $v_3^n$, $v_4^n$ and $v_5^n$) calculated in the $n^{\text{th}}$ time step. Therefore, the cumulative advancement distance of the wetting phase in each capillary at $t_{n+1}$ is:

$$x_i^{n+1} = x_i^n + v_i^n \Delta t \tag{15}$$

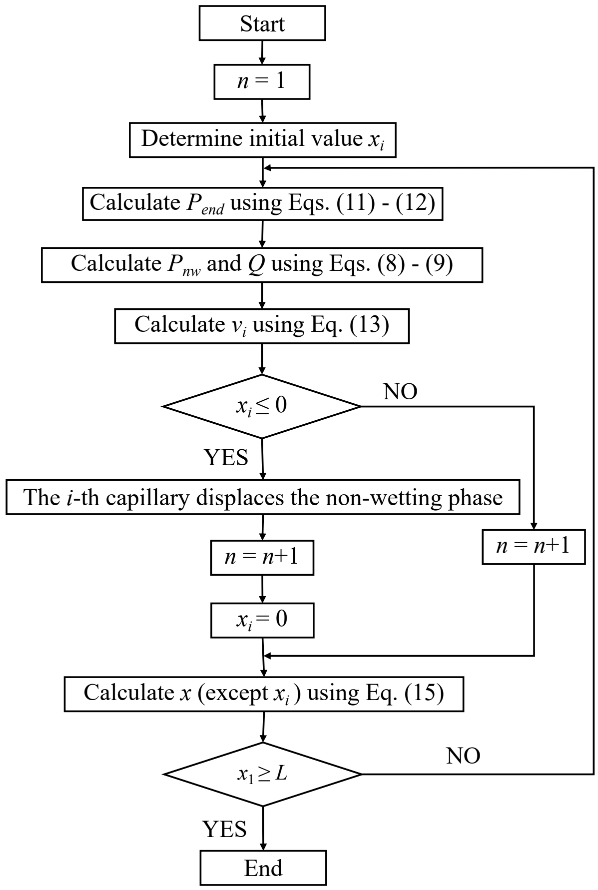


**Fig. 2**. Flowchart for solving the spontaneous imbibition model of five independent capillaries.

According to Eq. (15), the advancement distances ($x_1^{n+1}$, $x_2^{n+1}$, $x_3^{n+1}$, $x_4^{n+1}$ and $x_5^{n+1}$) of the wetting phase in the capillary at the $(n+1)^{\text{th}}$ time step are obtained. By substituting $x_1^{n+1}$, $x_2^{n+1}$, $x_3^{n+1}$, $x_4^{n+1}$ and $x_5^{n+1}$ into Eqs. (11) and (12), the $P_{end}$ at the $(n+1)^{\text{th}}$ time step is obtained. By bringing the calculated $P_{end}$ into Eqs. (8) and (9), it is possible to calculate the pressure $P_{nw1}$, $P_{nw2}$, $P_{nw3}$, $P_{nw4}$ and $P_{nw5}$ of the non-wetting phase fluid at the imbibition front in the capillary at the $(n+1)^{\text{th}}$ time step, the fluid rates $Q_1$, $Q_2$, $Q_3$, $Q_4$ and $Q_5$, and the velocities $v_1^{n+1}$, $v_2^{n+1}$, $v_3^{n+1}$, $v_4^{n+1}$ and $v_5^{n+1}$. According to the velocity of the $(n+1)^{\text{th}}$ time step, the wetting phase advancement distance at the $(n+2)^{\text{th}}$ time step can be obtained from Eq. (15).

Similarly, the advancement distance, advancement velocity, the pressure of wetting phase and non-wetting phase at the advancing front, the end pressure of the non-wetting phase fluid in the capillary, and the fluid flow in the capillary can be obtained for each time step in the process of fluid spontaneous imbibition of five capillaries.

In the process of spontaneous imbibition of the five capillaries, the capillaries start to displace the non-wetting phase when the wetting phase advancement distance in the capillary is less than or equal to 0 ($x \leq 0$). At this time, the advancement distance of the wetting phase in the capillary that discharges the non-wetting phase fluid is zero. Taking the non-wetting phase discharged from the fifth capillary as an example, the flow control equation of the fifth capillary can be obtained by substituting $x_5 = 0$ into Eqs. (8) and (9). Similarly, the solution can be obtained when other capillaries discharge non-wetting phase. The solution flowchart is shown in Fig. 2.

It is assumed that the starting time for imbibition in the initial state of the model is $t_1 = 1 \times 10^{-4}$ s (infinitely close to 0). The initial advancement distance of the wetting phase fluid in the five capillaries ($x_1^{n=1}$, $x_2^{n=1}$, $x_3^{n=1}$, $x_4^{n=1}$, $x_5^{n=1}$) needs to be given prior to be updated in the following time steps. According to the capillary pressure of each capillary, the relationship between the wetting phase advancement distances of the five capillaries in the initial state is $x_1 > x_2 > x_3 > x_4 > x_5$, and they all approach zero infinitely. It is worthwhile mentioning that because the displacement in the initial state ($n = 1$) is infinitely close to zero, it has little impact on the accuracy of the solution of the imbibition process. In this regard, the initial displacements are set to be $x_1^{n=1} = 1 \times 10^{-5}$ m, $x_2^{n=1} = 0.9 \times 10^{-5}$ m, $x_3^{n=1} = 0.8 \times 10^{-5}$ m, $x_4^{n=1} = 0.7 \times 10^{-5}$ m, and $x_5^{n=1} = 0.6 \times 10^{-5}$ m. The pressure $P_{in}$ at the inlet of the capillary tubes is set as 0 Pa during the infiltration process, and the time step $\Delta t$ is $1 \times 10^{-4}$ s.

In summary, without considering the effect of gravity, a spontaneous imbibition model in which the wetting phase displaces the non-wetting phase in five independent capillaries is established by using the Hagen-Poiseuille expression, capillary pressure formula, and mass conservation law. When the interval between time steps is very small, the propulsion velocity of the wetting phase or the discharge velocity of the non-wetting phase obtained in the previous time step can be used as the imbibition velocity under capillary pressure at the imbibition front in the next time step to update the quantities. In this way, the advancement distance, advancement velocity, the pressure of wetting phase and non-wetting phase at the advancing front, the bottom pressure of non-wetting phase fluid in the capillary, and the fluid flow in the capillary can be obtained at each time step in the process of fluid imbibition in the five capillaries.

## 4. Results and discussion

In this work, the process of spontaneous imbibition of the wetting phase fluid at one end of five capillaries with different diameters and displacement of non-wetting phase fluid in capillaries was simulated. The spatial-temporal characteristics of the advancement distance and velocity of the wetting phase in the capillary under different viscosity ratios, the water saturation ahead of the imbibition front, and the evolution of pressure at the end of the capillary over time were analyzed. Table 1 shows the relevant parameters of the imbibition model.

The capillary pressure is inversely proportional to the capillary radius, and the flow resistance is inversely proportional to the square of the capillary radius. Considering these combined effects, the smaller the capillary radius, the slower the imbibition speed (Mason and Morrow, 2013). However, the calculation results in this paper show that the wetting phase fluid preferentially enters the smaller capillary, and the non-wetting phase fluid is discharged from the larger capillary. In addition, for the water-absorbing capillaries, the advancement velocity of the interface in the smaller capillary is higher than

**Table 1**. Basic parameters of model.

| Parameter | Value |
|---|---|
| Capillary length (m) | $8 \times 10^{-3}$ |
| The first capillary diameter (m) | $0.20 \times 10^{-3}$ |
| The second capillary diameter (m) | $0.25 \times 10^{-3}$ |
| The third capillary diameter (m) | $0.30 \times 10^{-3}$ |
| The fourth capillary diameter (m) | $0.35 \times 10^{-3}$ |
| The fifth capillary diameter (m) | $0.40 \times 10^{-3}$ |
| The wetting phase viscosity (mPa·s) | 0.1, 1, 10 |
| The non-wetting phase viscosity (mPa·s) | 1 |
| Interfacial tension (mN/m) | 32 |

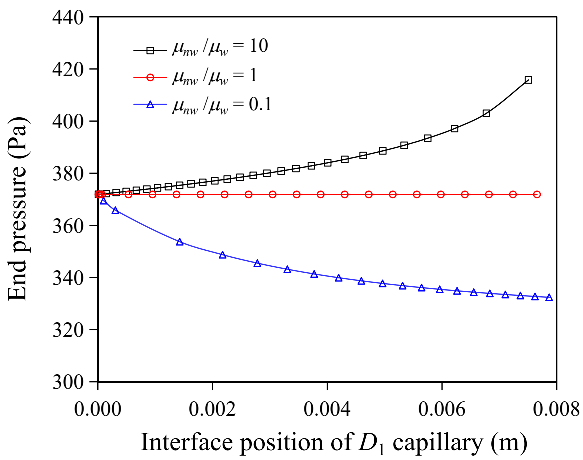


**Fig. 3**. Evolution of capillary end pressure at different viscosity ratios.

that in the larger capillary. Without additional displacement force (i.e., $P_{in} = 0$), it can be seen from Eqs. (9) and (13) that the advancement velocity increases with the decrease in capillary radius. Therefore, the wetting phase preferentially enters the smaller capillaries where it advances faster.

Firstly, end pressure is an important parameter for analyzing the imbibition characteristics of this mode, and this part is to analyze $P_{end}$ with different viscosity ratios. Fig. 3 shows the curves of capillary end pressure at different viscosity ratios, where the viscosity ratio is the ratio of the viscosity of the non-wetting phase to that of the wetting phase. Since the model begins calculation under the same initial displacements, the initial end pressure values of different viscosity ratios are the same as those from Eqs. (11) and (12).

For $\mu_{nw}/\mu_w = 1$, with the capillaries absorbing the wetting phase and discharging the non-wetting phase, the total viscosity of the fluid filled with the capillaries is constant. It is clear that the resistance of the whole imbibition process remains unchanged, and the model does not exert additional displacement force. Therefore, the end pressure is constant throughout the process (red curve in Fig. 3). When the viscosity of the non-wetting phase is constant, the viscosity ratio is altered by changing the viscosity of the wetting phase. When the viscosity of the wetting phase is greater than that of the non-wetting phase (i.e., $\mu_{nw}/\mu_w < 1$), the viscous resistance of the wetting phase fluid flow continues to rise. The reason is that the viscosity resistance is proportional to the viscosity, and the flow distance of the wetting phase continues to increase with the flow in this model. In this way, the pressure consumed by the wetting phase flow increases, and the pressure decreases as the fluid reaches the end of the capillary. Consequently, the end pressure decreases continuously for $\mu_{nw}/\mu_w = 0.1$ (blue curve in Fig. 3). Conversely, the viscous resistance of wetting phase fluid flow continues to decrease when $\mu_{nw}/\mu_w > 1$. The pressure consumed by the wetting phase flow decreases, and the pressure increases as the fluid reaches the end of the capillary. Therefore, the end pressure increases continuously for $\mu_{nw}/\mu_w = 10$ (black curve in Fig. 3). The above are the main characteristics of $P_{end}$ at different viscosity ratios during the flow process.

Based on the analysis of end pressure, the flow characteristics in each capillary under different viscosity ratios are analyzed (Fig. 4). For $\mu_{nw}/\mu_w = 1$, the resistance and end pressure of the whole imbibition process remain constant (Fig. 3). Therefore, the velocity of fluid in each capillary remains unchanged, as shown in Fig. 4(b). In addition, the end pressure is higher than the capillary pressure $P_{c4}$, which causes the capillary with diameter $D_4$ to become an oil drainage channel (i.e., $v_4 < 0$ in Fig. 4(b)).

For $\mu_{nw}/\mu_w < 1$, the viscous resistance of wetting phase fluid flow continues to increase, and the model does not exert additional displacement force. Consequently, the overall imbibition rate of the model consistently slows down. Although the end pressure decreases continuously, $P_{end}$ is initially greater than $P_{c4}$. As the flow progresses, the capillary with diameter $D_4$ will change from an oil drainage channel to a water absorption channel (i.e., $v_4$ in Fig. 4(a)). The advancement velocity of the interface increases due to the pressure difference formed by capillary pressure in the tube after the change of channel type. Subsequently, it decreases as the viscous resistance increases. Regardless of how the $P_{end}$ decreases, it is greater than $P_{c5}$; therefore, the capillary with diameter $D_5$ is always the oil drainage channel in this model, whereas the channel type of capillary $D_4$ is variable.

In the process of imbibition, when the viscosity of the non-wetting phase is greater than the viscosity of the wetting phase, the viscous resistance of wetting phase fluid flow continues to decrease and the overall displacement velocity increases continuously. Therefore, the imbibition velocity increases slightly at the early stage of imbibition, and it increases greatly in the later period. For the capillary with diameter $D_1$, the capillary pressure is the largest, the influence of end pressure is small, and there are more wetting phases in the tube. Thus, the advancement resistance of the wetting phase in the first capillary is greatly reduced, resulting in a significant increase in the advancement velocity in the later stage (i.e., $v_1$ in Fig. 4(c)). For $D_2$ and $D_3$, the capillary pressure is smaller. The increasing advancement resistance with the increasing end pressure is greater than the decreasing resistance with more and more wetting phases in the tube. Therefore, the

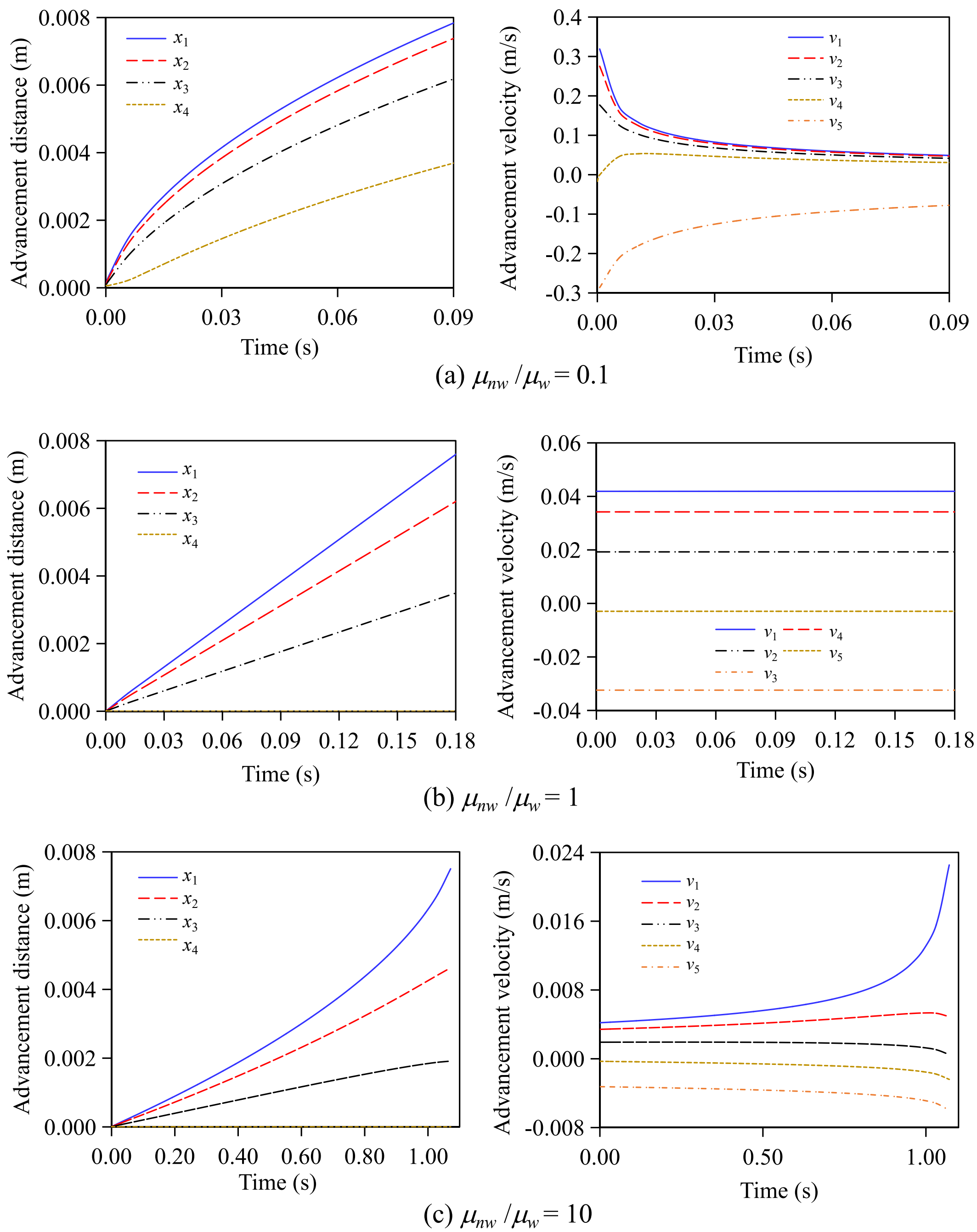


**Fig. 4**. Advancement distance and velocity curve in capillary tubes at different viscosity ratios (the direction of wetting phase flow into the capillary is positive; the direction of non-wetting phase flowing out of the capillary is negative).

advancement velocity in the capillaries with diameters $D_2$ and $D_3$ decreases in the later stage. Since the end pressure of the capillary tube is greater than the capillary pressure $P_{c4}$, the non-wetting phase is discharged from the capillaries with diameters $D_4$ and $D_5$.

In the process of imbibition, it is necessary to study the heterogeneity of how the imbibition front advances at different viscosity ratios. Fig. 5 presents the curves of water saturation ahead of the imbibition front at different viscosity ratios. When this saturation is high, the difference in the advancement of wetting phase in each capillary is small, meaning that the advancement is more uniform. On the other hand, the advancement becomes uneven when the water saturation is low. Thus, the water saturation ahead of the imbibition front can directly reflect the heterogeneity of imbibition, making it easier to study the heterogeneity of the advancement of the imbibition front.

As the wetting phase advances, the end pressure remains unchanged and the flow velocity of fluid in each capillary is constant for $\mu_{nw}/\mu_w = 1$, as shown in Fig. 4(b). Therefore, the

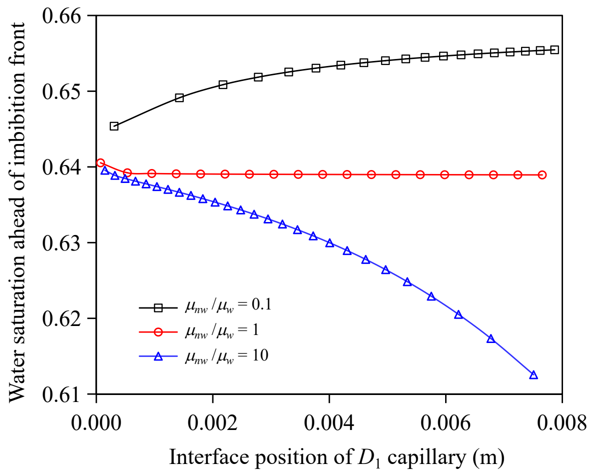


**Fig. 5**. Curves of water saturation ahead of imbibition front at different viscosity ratios (this water saturation refers to the total water saturation of five capillaries ahead of the imbibition front of the smallest capillary).

water saturation of the advancing front does not change (red curve in Fig. 5). The heterogeneity of the advancement of imbibition front also remains unaltered. For $\mu_{nw}/\mu_w < 1$, the viscous resistance of wetting phase fluid flow continues to increase and the velocity of displacement of the non-wetting phase becomes smaller and smaller as the wetting phase advances during the process of imbibition. Therefore, as shown in Fig. 4(a), the difference in advancement velocity becomes gradually smaller. Then, the interface advancement is more and more uniform, and the water saturation of the advancing front becomes increasingly larger. For $\mu_{nw}/\mu_w > 1$, as the wetting phase advances, the viscous resistance of wetting phase fluid flow continues to decrease. In the water absorbing capillaries, the difference between the flow velocity of the wetting phase in small capillaries and that in other capillaries is growing, as shown in Fig. 4(c). Therefore, the difference between the advancement of the wetting phase and the non-wetting phase interface becomes gradually larger, and the water saturation of the advancement front becomes gradually smaller.

When comparing the changes in the water saturation the imbibition front with three different viscosity ratios, the water saturation decreases when $\mu_{nw}/\mu_w > 1$. It is shown that the wetting phase advances more and more unevenly when the viscosity of the wetting phase is less than that of the non-wetting phase. This is because the viscous resistance of wetting phase fluid flow continues to decrease compared with the scenario of $\mu_{nw}/\mu_w = 1$. The difference in capillary pressure allows the small capillary to advance very quickly. Therefore, when $\mu_w < \mu_{nw}$, the heterogeneity in the advancement of interfaces becomes stronger and the water saturation ahead of the imbibition front becomes smaller. In the same way, the interface advances more and more uniform for $\mu_w > \mu_{nw}$.

## 5. Conclusions

1) When the viscosity ratio is greater than 1, the imbibition rate becomes increasingly faster with the process of imbibition. When the viscosity ratio is less than 1, the imbibition speed becomes slower with the advancement of imbibition.
2) The higher the viscosity ratio of non-wetting phase to wetting phase, the more oil discharge channels, that is, the smaller capillaries are more likely to discharge oil.
3) The higher the viscosity ratio, the greater the end pressure of capillary in the process of imbibition. Meanwhile, the lower the viscosity ratio, the smaller the end pressure of capillary. When the viscosity ratio is greater than 1, the end pressure increases with the advancement of imbibition. Meanwhile, when the viscosity ratio is less than 1, the end pressure decreases with the imbibition progressing.
4) The smaller the viscosity ratio, the more uniform the interface advancement between different capillaries, and the greater the water saturation ahead of the imbibition front; the larger the viscosity ratio, the greater the difference in advancement distances, and the smaller the water saturation ahead of the imbibition front.


## Acknowledgements

This project was supported by the National Natural Science Foundation of China (Nos. 51804284, 51874262).


## Conflict of interest

The authors declare no competing interest.



## References


Abd, A. S., Elhafyan, E., Siddiqui, A. R., et al. A review of the phenomenon of counter-current spontaneous imbibition: Analysis and data interpretation. Journal of Petroleum Science and Engineering, 2019, 180: 456-470.

Bourblaux, B. J., Kalaydjian, F. J. Experimental study of cocurrent and countercurrent flows in natural porous media. SPE Reservoir Engineering, 1990, 5(3): 361-368.

Cai, J., Jin, T., Kou, J., et al. Lucas-Washburn equation-based modeling of capillary-driven flow in porous systems. Langmuir, 2021, 37(5): 1623-1636.

Cai, J., Perfect, E., Cheng, C., et al. Generalized modeling of spontaneous imbibition based on Hagen-Poiseuille flow in tortuous capillaries with variably shaped apertures. Langmuir, 2014, 30(18): 5142-5151.

Cai, J., Yu, B. A discussion of the effect of tortuosity on the capillary imbibition in porous media. Transport in Porous Media, 2011, 89: 251-263.

Cai, J., Yu, B., Zou, M., et al. Fractal characterization of spontaneous co-current imbibition in porous media. Energy & Fuels, 2010, 24(3): 1860-1867.

Cheng, Z., Gao, H., Ning, Z., et al. Inertial effect on oil/water countercurrent imbibition in porous media from a pore-scale perspective. SPE Journal, 2022, 27(3): 1619-1632.

Dong, M., Dullien, F. A. L., Dai, L., et al. Immiscible displacement in the interacting capillary bundle model part

I. Development of interacting capillary bundle model. Transport in Porous Media, 2005, 59: 1-18.
Dong, M., Dullien, F. A. L., Dai, L., et al. Immiscible displacement in the interacting capillary bundle model part II. Applications of model and comparison of interacting and non-interacting capillary bundle models. Transport in Porous Media, 2006, 63: 289-304.
Foley, A. Y., Nooruddin, H. A., Blunt, M. J. The impact of capillary backpressure on spontaneous counter-current imbibition in porous media. Advances in Water Resources, 2017, 107: 405-420.
Gong, Y., Piri, M. Pore-to-core upscaling of solute transport under steady-state two-phase flow conditions using dynamic pore network modeling approach. Transport in Porous Media, 2020, 135(1): 181-218.
Gong, Y., Sedghi, M., Piri, M. Dynamic pore-scale modeling of residual trapping following imbibition in a rough-walled fracture. Transport in Porous Media, 2021, 140(1): 143-179.
Gorce, J. B., Hewitt, I. J., Vella, D. Capillary imbibition into converging tubes: Beating Washburn's law and the optimal imbibition of liquids. Langmuir, 2016, 32(6): 1560-1567.
Haugen, Å., Fernø, M. A., Mason, G., et al. Capillary pressure and relative permeability estimated from a single spontaneous imbibition test. Journal of Petroleum Science and Engineering, 2014, 115: 66-77.
Kim, K., Kim, M., Oh, J. Core-scale investigation of the effect of heterogeneity on the dynamics of residual and dissolution trapping of carbon dioxide. Journal of Hydrology, 2021, 596: 126109.
Mason, G., Fischer, H., Morrow, N. R., et al. Correlation for the effect of fluid viscosities on counter-current spontaneous imbibition. Journal of Petroleum Science and Engineering, 2010, 72(1-2): 195-205.
Mason, G., Morrow, N. R. Developments in spontaneous imbibition and possibilities for future work. Journal of Petroleum Science and Engineering, 2013, 110: 268-293.
Meng, Q., Liu, H., Wang, J. A critical review on fundamental mechanisms of spontaneous imbibition and the impact of boundary condition, fluid viscosity and wettability. Advances in Geo-Energy Research, 2017a, 1(1): 1-17.
Meng, Q., Liu, H., Wang, J. Effect of viscosity on oil production by cocurrent and countercurrent imbibition from cores with two ends open. SPE Reservoir Engineering, 2017b, 20(2): 251-259.
Morrow, N. R., Mason, G. Recovery of oil by spontaneous imbibition. Current Opinion in Colloid & Interface Science, 2001, 6(4): 321-337.
Nooruddin, H. A., Blunt, M. J. Analytical and numerical investigations of spontaneous imbibition in porous media. Water Resources Research, 2016, 52(9): 7284-7310.
Pooladi-Darvish, M., Firoozabadi, A. Cocurrent and countercurrent imbibition in a water-wet matrix block. SPE Journal, 2000, 5(1): 3-11.
Qin, C. Z., Wang, X., Hefny, M., et al. Wetting dynamics of spontaneous imbibition in porous media: From pore scale to darcy scale. Geophysical Research Letters, 2022, 49(4): e2021GL097269.
Ruth, D., Bartley, J. A perfect-cross-flow model for two phase flow in porous media. Paper SCA2002-05 Presented at the International Society of Core Analysts Annual Meeting, Monterey, CA, USA, May, 2002.
Shen, A., Liu, Y., Farouq, S. M. A model of spontaneous flow driven by capillary pressure in nanoporous media. Capillarity, 2020, 3(1): 1-7.
Unsal, E., Mason, G., Ruth, D. W., et al. Co- and counter-current spontaneous imbibition into groups of capillary tubes with lateral connections permitting cross-flow. Journal of Colloid and Interface Science, 2007, 315(1): 200-209.
Wang, J., Dong, M. Trapping of the non-wetting phase in an interacting triangular tube bundle model. Chemical Engineering Science, 2011, 66(3): 250-259.
Wang, Z., Li, H., Lan, X., et al. Formation damage mechanism of a sandstone reservoir based on micro-computed tomography. Advances in Geo-Energy Research, 2021, 5(1): 25-38.
Washburn, E. W. The dynamics of capillary flow. Physical Review, 1921, 17(3): 273-283.
Xiao, J., Luo, Y., Niu, M., et al. Study of imbibition in various geometries using phase field method. Capillarity, 2019, 2(4): 57-65.
Yang, Z., Liu, X., Li, H., et al. Analysis on the influencing factors of imbibition and the effect evaluation of imbibition in tight reservoirs. Petroleum Exploration and Development, 2019, 46(4): 779-785.
Zhang, X., Morrow, N. R., Ma, S. Experimental verification of a modified scaling group for spontaneous imbibition. SPE Reservoir Engineering, 1996, 11(4): 280-285.
Zhao, J., Qin, F., Fischer, R., et al. Spontaneous imbibition in a square tube with corner films: Theoretical model and numerical simulation. Water Resources Research, 2021, 57(2): e2020WR029190.
Zhou, Y., Pu, H., Zhong, X., et al. Visualized experiment of the imbibition oil recovery for the nano-particles in Hele-Shaw model. Petroleum Geology & Oilfield Development in Daqing, 2019, 38(6): 46-51. (in Chinese)